2021

Efficient Simulation Method for Parallel Tube Evaporators for Vehicle Battery Cooling

Bernhard Einberger
Graz University of Technology

Christoph Zainer
Graz University of Technology

Andreas Ennemoser
AVL List GmbH

Sebastian Möller
Virtual Vehicle Research GmbH

Andreas Egger
Graz University of Technology, egger@ivt.tugraz.at

See next page for additional authors

Efficient Simulation Method for Parallel Tube Evaporators for Vehicle Battery Cooling

Bernhard EINBERGER[2]*, Christoph ZAINER[1], Andreas ENNEMOSER[2], Sebastian MÖLLER[3], Andreas EGGER[1], Michael LANG[1]

[1]Graz University of Technology, Institute of Internal Combustion Engines and Thermodynamics,
Inffeldgasse 19, 8010 Graz, Austria
zainer@ivt.tugraz.at
egger@ivt.tugraz.at
michael.lang@ivt.tugraz.at

[2]AVL List GmbH,
Hans-List-Platz 1, 8010 Graz, Austria
bernhard.einberger@avl.com
andreas.ennemoser@avl.com

[3]Virtual Vehicle Research GmbH,
Inffeldgasse 21a, 8010 Graz, Austria
sebastian.moeller@v2c2.at

*Corresponding Author

ABSTRACT

Due to its size, the cooling of a vehicle battery by means of a refrigeration system has to be implemented e.g. via parallel evaporator tubes. After the throttle, the two-phase refrigerant flow must be uniformly distributed into several cooling channels so that uniform cooling can be achieved throughout the entire volume. The simulation of the three-dimensional effects in the distributor and also in the collector of an evaporator with several parallel evaporator tubes can only be done by computational fluid dynamics (3D CFD). However, the 3D CFD simulation of the evaporator is time consuming and can be replaced by a 1D calculation applying simple correlations for pressure losses and heat transfer coefficients (HTCs). The 1D model approach is implemented by a script that runs within the commercial software of the industrial partner for a parallel tube evaporator geometry.
The CFD simulation is based on a Eulerian multiphase approach where both phases are modelled as continuous fluids and all conservation equations are solved for each of these phases. The evaporator tubes are discretised in the direction of the tube in order to get the distribution of the variables in longitudinal direction. The used refrigerant is R134a.
In this work, an evaporator consisting of a distributor, a collector and four parallel evaporator tubes that were led at right angles to them was investigated. All these components are located in a plane. This geometry has been chosen in accordance with tests carried out.
The focus of this paper is the coupling method, the simplification that has been made and the efficiency of the simulation. A comparison between simulation and test bench measurements shows deviations in the total mass flow distribution in the order of less than 10%. Liquid and vapor mass distribution show larger deviations in the order of 20-50% in different operating conditions. Possible improvements can be achieved by varying influencing factors in the CFD-simulation, e.g. the droplet diameter. Finally, the results are analysed for the variation of two parameters. The method is also applicable to geometric variations of heat exchangers.

1 INTRODUCTION

Due to the increasing electrification of the automotive sector, the topic of thermal management of the associated components in the vehicle, such as the power electronics or the batteries, is becoming more and more important. The batteries in particular produce a large amount of heat to be dissipated e.g. during fast charging which makes an effective cooling system essential. Due to the space and weight limitations in mobile applications, cooling circuits with parallel evaporator tubes are the obvious choice. The investigation of the evaporation process in such a heat exchanger by means of a 3D CFD simulation is demanding. It is based on a numerical and, thus, computationally

time-intensive effort to represent the multiphase flow and the associated physical effects such as mass, momentum and heat transfer. To enable an efficient simulation, the flow effects must be simplified by models and approximations, which in turn can lead to deviations and inaccuracies.

In this paper, an approach is presented that allows a fast assessment of the multiphase flow of R134a in a heat exchanger with parallel evaporator tubes. To make the simulation as efficient as possible, a 1D / 3D coupling has been chosen. The aim is to simulate the distributor and collector using 3D CFD and to map the physical effects in the evaporator tubes with a self-programmed 1D model in order to keep the numerical effort for the phase transition low. The simulation is carried out with the software AVL FIRE (version R2018.a), in which the 1D model is programmed as a user-defined function (a so-called global formula) using a C code. The simplest possible boundary conditions of the 3D CFD model, e.g. velocity, temperature and vapor quality at the inlet and static pressure at the outlet, are applied. This leads to a time-efficient numerical procedure that allows the variation of different geometries and boundary conditions.

The 3D simulation of the distributor is necessary to understand the distribution of the liquid and gaseous phases inside and to obtain the inlet conditions of the evaporator tubes. The two-phase flow in the manifold is assumed to be adiabatic. The conditions at the four outlets of the manifold are read out and transferred to a 1D code as input conditions. In the 1D model, the most important physical effects such as pressure loss and heat transfer are taken into account by correlations and, thus, the evaporation process is calculated in a simplified way. Several different correlations for calculating the heat transfer coefficient and the pressure loss are included in this code and can be selected. These correlations are mainly based on experimental investigations, as can be read in numerous relevant papers listed in Bell (2016-2018) and Bell (2016-2019). The high number of different approaches to represent heat transfers or pressure losses show the difficulty of describing multiphase flows with phase transitions. After the 1D calculation of the evaporator tubes, the outlet conditions of the four lines are transferred as inlet boundary conditions to the collector, which is then simulated adiabatically using 3D CFD. Due to the short calculation time of this evaporator modelling, which is mainly based on the cell number of the 3D parts, a DOE investigation is finally possible.

The plausibility and informative value of the 1D / 3D coupling model was examined on the basis of various influencing factors such as inlet mass flow, inlet vapor quality, inclination angle of the evaporator, average droplet diameter of the dispersed phase and the various pressure loss correlations. Some of these variations are compared with the measured values from the test rig and discussed. It should be noted that the experimental tests were only partially carried out due to the resources available.

2 PARALLEL TUBE HEAT EXCHANGER

Figure 1 shows the heat exchanger to be examined consisting of a distributor, a collector and four parallel evaporation tubes (evap_1 to evap_4) with a length of 800 mm and a distance in between of 90 mm. These tubes are led at right angles from the distributor to the collector with an inner diameter of 2 mm and an outer diameter of 4 mm. The inner diameter of the distributor pipe is 8 mm respectively 14 mm in the collector.

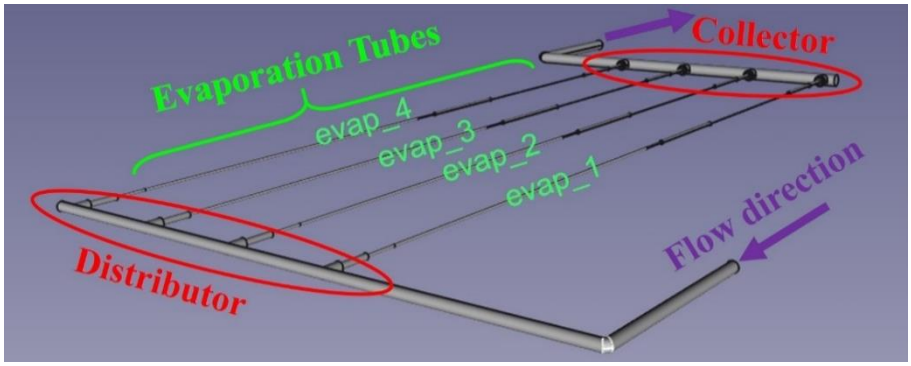

Figure 1: Components of the heat exchanger

Due to the variable positions of a vehicle in operation, different inclinations of the evaporator can occur as shown in Figure 2. This tendency must be taken into account when examining the evaporation process due to the effects of gravity on the mass distribution. The angle φ of inclination is defined positively if the direction of the inflow is upward against gravity. In the experimental study, a rotation around the distributor axis was also investigated, but this is not shown here.

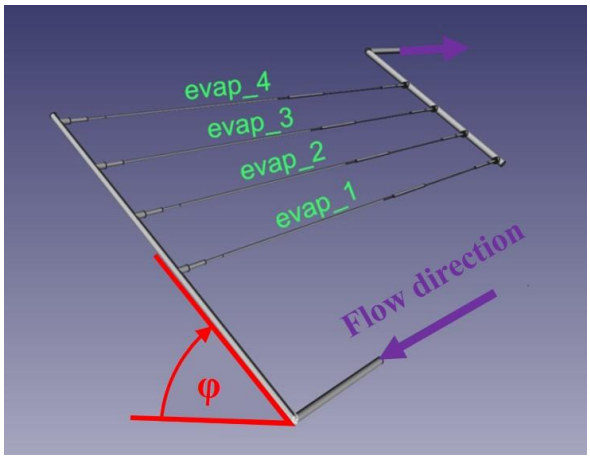

Figure 2: Rotation of the evaporator

3 SIMULATION MODEL

The focus of this investigation is on the 1D / 3D coupling of the CFD simulation for the flow processes. The basic approaches such as the solver settings, the boundary conditions and correlations used as well as the coupling method of the numerical model are of particular interest and have a significant influence on the simulation.

3.1 Solver settings and multiphase approach

As already mentioned, the CFD simulation is carried out in AVL FIRE, which uses the finite volume approach to solve the conservation equations. A transient simulation is performed as the 1D / 3D coupling is carried out via an iterative procedure with a stepwise approximation to the correct steady-state solution. The global boundary conditions are the inlet conditions of the manifold and the outlet conditions of the collector. Inner boundary conditions denote the conditions at the interfaces between the distributor or collector to the evaporator tubes. The k-ε model with a hybrid wall treatment is used as the turbulence model, as well as the standard wall function for the wall heat transfer model. Slightly decreased sub-relaxation factors for momentum, pressure and energy are used, slowing down convergence but improving stability to avoid numerical divergence. Furthermore, gravitational body force is included in the calculation to account for the influence of different rotations of the evaporator on the overall evaporation process.

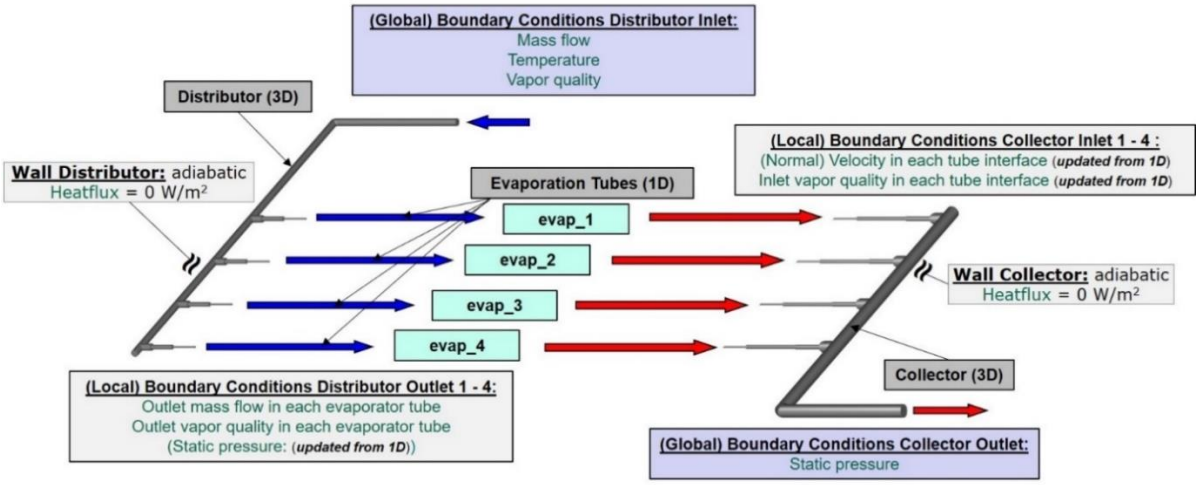

Figure 3: Scheme and boundary conditions of the simulation model

A continuous phase (main phase that pushes or pulls the dispersed phase; in this case the vapor phase) and a dispersed phase (in this case the liquid phase) are defined. This is important to describe the momentum interfacial exchange that considers drag forces and turbulent dispersion forces. These reciprocal influences pull the dispersed phase from areas with high to low volume fractions. Interfacial momentum exchange can be very different depending on the application, which is why different models exist. Equation (1) describes an approach for the momentum exchange applied on the continuous phase respectively dispersed phase and can be found in detail in the AVL-FIRE Eulerian Multiphase Documentation (2018).

$$M_c = C_D \frac{1}{8} \rho_c A_i |v_r| v_r + C_{TD} \rho_c k_c \nabla \alpha_d = -M_D \tag{1}$$

In equation (1), C_D is the drag coefficient modelled, which is a function of the flow state and depends on the droplet / bubble Reynolds number and therefore on the droplet diameter, on the relative velocity between the dispersed and the continuous phase as well as the viscosity of the continuous phase. A_i is the interfacial area density, ρ_c the density and C_{TD} a constant to take dispersion forces into account. These are set by the exchange model. $\nabla \alpha_d$ is the difference between the volume fractions and k_c the thermal conductivity of the continuous phase. Equation (2) describes the relative velocity between the two phases.

$$v_r = v_D - v_C \tag{2}$$

A critical issue is that different flow processes can occur in multiphase flows, such as bubble flow, plug flow or ring flow. These can be looked up eg. in the VDI Wärme Atlas in literature Stephan et al. (2018). It is important to note that the AVL-FIRE CFD-Solver Documentation (2018) and the AVL-FIRE Eulerian Multiphase Documentation (2018) do not assess the accuracy of the available models.

3.2 1D multiphase correlations

As mentioned before, the physical processes in the evaporator tubes are mathematically described in the 1D model using different correlations. The input states of the evaporator tubes are retrieved from the 3D CFD simulation of the distributor. The most important effects to be described by correlations are the heat transfer coefficient and the pressure loss.

3.2.1 Heat transfer coefficient correlations

The HTC correlations are taken from the heat transfer homepage of Bell (2016-2019) where further literature and the restrictions for these approaches are available. The calculation of the heat transfer coefficient requires either the excess temperature T_e (difference between wall temperature and fluid temperature) or a heat source q. Two HTC correlations are incorporated into the 1D model, first according to Li and Wu (2010) and second according to Lazarek and Black (1982).

The correlation according to Li and Wu (2010) suggests heat transfer coefficients at any flow orientation at film boiling conditions. It is assumed that the flow is at saturation condition and tests were carried out for pipe diameters from 0.19 mm to 3.1 mm with twelve different fluids. The correlation is given according to equations (3) and (4), where the liquid Reynolds number, the Bond number and the Boiling number are used.

$$\alpha = 334 * Bg^{0.3} (Bo \cdot Re_l^{0.36}) * \frac{k_l}{D} \tag{3}$$

$$Re_l = \frac{G(1-x)D}{\mu_l} \tag{4}$$

Lazarek and Black (1982) developed a correlation for film boiling at saturation conditions. This approach is especially suitable for the calculation of vertical pipes with flow direction upwards or downwards. The correlation does not take vapor quality and vapor properties into account, the entire flow is assumed to be liquid for the calculation of the Reynolds number. Therefore, no other properties of gas are required. Equations (5) and (6) show the correlations.

$$\alpha = 30\, Re_{lo}^{0.857}\, Bg^{0.714} \frac{k_l}{D} \tag{5}$$

$$Re_{lo} = \frac{G_{tp} D}{\mu_l} \tag{6}$$

3.2.2 Pressure loss correlations

All pressure loss correlations are based on test data which are converted to empirical equations. The existing pressure loss correlations differ in the assumptions for the flow and other relevant properties for the pressure loss. Most of the following authors in Table 1 use equation (7) to calculate the pressure loss, the variables used vary based on the assumptions made.

$$\Delta p = \Delta p_{lo} {\phi_{lo}}^2 \tag{7}$$

The different correlations and some comments to each of them are listed in Table 1 with the exception of the Müller-Steinhagen and Heck correlation. All of these correlations were found on the fluids homepage of Bell (2016-2018) where further literature on the individual models is available.

Table 1: Overview of implemented pressure loss correlations

Correlation name	Comments	Reference
Friedel	For vertical upflow and horizontal flow; mean errors in order of 40%, tube diameters of 4mm	Friedel (1979)
Zhang and Webb	vapor quality from 0 to 1; tube diameters from 2.13 mm to 5.25 mm; mean deviation of 11.5%	Zhang and Webb (2001)
Lockhart and Martinelli	For horizontal flow; very popular; various turbulent-laminar combinations	Lockhart and Martinelli (1949) Chishom (1967) Cui and Chen (2010)
Kim and Mudawar	Critical Reynolds number of 2000; hydraulic diameters from 0.0695 mm to 6.22 mm; vapor quality from 0 to 1	Kim and Mudawar (2012) Kim and Mudawar (2014)

Müller-Steinhagen and Heck

The only correlation in this paper not using these equations is the one according to Müller-Steinhagen and Heck (1986). This approach can be used for vapor qualities from 0 to 1 and can be easily implemented. Equations (8) and (9) describe the correlations.

$$\Delta p_{tp} = G_{MSH}(1-x)^{1/3} + \Delta p_{go} x^3 \tag{8}$$

$$G_{MSH} = \Delta p_{lo} + 2\left[\Delta p_{go} - \Delta p_{lo}\right] x \tag{9}$$

3.3 Coupling method

The 3D CFD parts (manifold and collector) must be coupled with the programmed 1D model of the evaporator tubes. The coupling of the 1D and 3D domains means the conservation of mass, momentum and energy must be satisfied at all common interfaces. Therefore, the resulting mass flow, vapor quality, pressure, velocity, etc. must ultimately be the same at an interface. First, the 3D calculation of the distributor and the collector is explained, then the 1D model of the evaporator tubes and afterwards the iterative simulation process of the entire system. Finally, the assumptions and simplifications made and their expected deviations on the results are discussed.

3.3.1 3D setup of distributor and collector in AVL FIRE

The same two types of boundary conditions are used in 3D for the collector and the manifold. At the inlet, a constant normal velocity and a common temperature are selected for both phases, resulting in the corresponding mass flow. A static pressure is applied at the outlet, which represents the evaporation pressure. For each 1D evaporator tube, an inlet face selection and an outlet face selection must be defined as interfaces between the 3D and 1D domains.

The walls of the 3D domain are adiabatic. Two parameters which are difficult to describe should be mentioned here. One is the droplet / bubble diameter and the other is the rotation of the test rig. The effects of these two parameters on the mass distribution are discussed in chapter 4. AVL FIRE does not directly support the simulation of a range of droplet / bubble diameters, but multiple phases with different pronounced droplet / bubble diameters can be defined to create a range. Selecting different diameters improves the accuracy of the simulation, but was not done in this project due to the focus on the coupling method. Therefore, a constant droplet / bubble diameter was used.

3.3.2 1D model of evaporator tubes

AVL FIRE supports an environment for integrating extended functionalities using user coded functions called global formulas in the programming language C. The 1D model has been programmed as such a global formula. 1D means that the state variables only change in flow direction, in this case being the tube direction. The tube is sub-divided into a number n of sub-volumes for spatial discretization using the finite volume method. Due to the 1D assumption, phase separation and other 3D flow effects cannot be considered in this domain. This results in a constant heat flux over the surface of a volume element. The state in each element (1, 2, ..., n) is described with constant variables and a uniform velocity (x_1, α_1, p_1, ...). From volume to volume, the empirical equations for pressure loss and heat transfer coefficient, which modify the state variables in the elements, are solved.
As mentioned before, the inlet boundary conditions of the 1D domain are provided by the 3D CFD calculated values at the distributor outlets. The state at the outlet of the 1D domain is the inlet boundary condition at the interface to the collector.

3.3.3 Simulation workflow

In a first step, both 3D domains are calculated synchronously for one time step. Due to the constant global boundary conditions (inlet of the distributor and outlet of the collector), the transient simulation finally leads to a stationary converged solution. The concept of transient simulation is used to fit the results of the 1D models to those of the two 3D areas. The 3D simulation of the distributor is carried out for different static pressures at the four interfaces to the evaporator tubes. This results in four different mass flows, vapor qualities, velocities etc. at each of the four outlets.
The 3D simulation of the collector is carried out with the same four mass flows of the distributor outlets. The inlet conditions of the four inlets of the collector are the outlet conditions at the last element of each of the four 1D resolved tubes. The 3D simulation of the collector results in a static pressure at each of the four inlets.

In the evaporator tubes the 1D model calculates the flow in three partial steps: The first partial step reads the boundary conditions from the 3D domain at the distributor outlet and transfers it to the 1D model. The second partial step is the consecutive calculation of the heat transfer and the pressure drop for each element in flow direction. In the final step the outlet boundary of the last element of each tube is transferred to the inlet boundary conditions at the four inlets of the collector. As the mass flow does not change for a stationary solution it can directly be taken from the 3D results of the distributor. The temperature or the vapor quality and the pressure is a result of the 1D calculation. Finally the pressure at the outlet (the final element in flow direction) of every tube has to be compared to the 3D simulated pressure level at each collector inlet. For a converged solution the pressure values at these interfaces must be the same. The adjustment of these two pressure levels is carried out in an iterative approach. If the pressure at the oulet of a 1D tube is lower than the 3D pressure result at the corresponding inlet of the collector the mass flow of this tube is too high. Therefore the pressure at the outlet of the distributor for this tube has to be increased which results in a lower outflow through this interface. The correction of the pressure at the four outlets must be carried out in small steps in order to prevent numerical oscillations or a crash of the procedure.

3.3.4 Assumptions and Simplifications

The present simulation is based on some simplifications that draw some conclusions. First, constant vapor and liquid properties in the 3D domain are assumed. Constant fluid properties mean that superheated vapor is treated like saturated vapor, resulting in incorrect enthalpy fluxes. To avoid this, variable fluid properties can be integrated with formulas, but this can lead to higher computational effort and to numerical problems due to discontinuities in the mathematical equations. This simplification only concerns the collector.
Furthermore, no mass interfacial exchange is taken into account in the 3D domain. This means that no evaporation or condensation is considered in the simulation of these domains, which will occur in reality. For example, pressure losses cause evaporation.
The 1D domain uses empirical equations, which according to their authors are only valid for a certain application range. This means that the application is very limited to the testbed testmatrix of each correlation.
The flow is assumed to be incompressible, which is a good assumption for small Mach numbers and therefore useful for this application. If backflows in the evaporation areas occur, they are suppressed, as this can lead to numerical instabilities in the present 1D model. In addition, a spectrum of droplet / bubble diameters occurs in reality, which is assumed in the simulation by a constant droplet / bubble diameter.

3.4 Parameter variations tested in simulation

The following parameters are varied in the simulation to analyse their impact on the mass distribution:

- Different pressure correlations according to chapter 3.2
- Comparison of mass distribution and pressure loss on big header rotations (horizontal, 15°, -15°, 30°)
- Different droplet / bubble diameters (500 µm, 25 µm, 10 µm, 1 µm, 0,1 µm)
- Small rotations (5°, 1°, 0,2°)

4 RESULTS

As an example, the variation of two parameters listed in chapter 3.4 and their influence on the results are compared with practical measurements of the test rig. At this point, reference is made to Kollik et al. (2021) which deals with the experimental investigation of the liquid and vapor mass flows of the parallel tube evaporator presented.
It should be noted that the present paper does not go into detail about the results, but primarily aims to show how the coupling was carried out and which correlations can be used for multiphase applications.

4.1 Comparison of different droplet / bubble diameters

As mentioned before, the selection of the droplet / bubble diameter has an impact on the mass distribution of the evaporator. In each of the presented simulations, these diameters are set constant to the values listed below the diagrams. Figure 4 and Figure 5 show the distribution of the total (left side), liquid (middle) and vapor mass flow (right side) in the four evaporator tubes. In this case, the total inlet mass flow into the distributor is 11 kg/h with a quality of 0.32. The testbed-data is used for reference. In the presented simulations the pressure loss correlation of Müller-Steinhagen and Heck (1986) and the HTC correlation of Li and Wu (2010) have been applied.

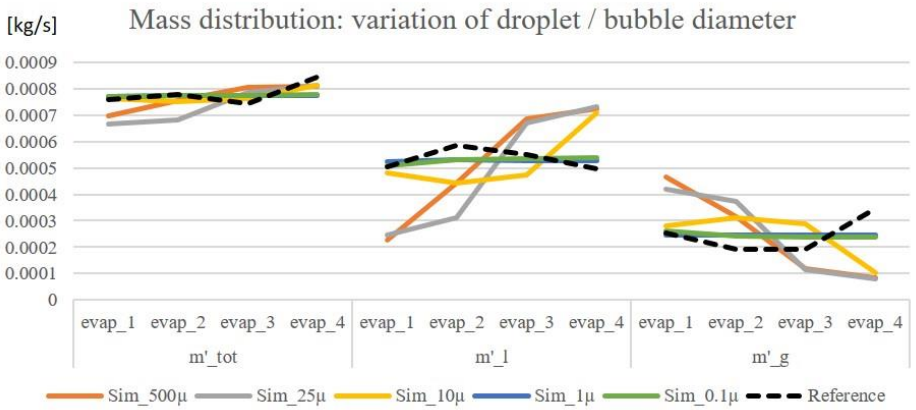

Figure 4: Mass flow distribution (total, liquid and gaseous) due to different droplet / bubble diameters (1)

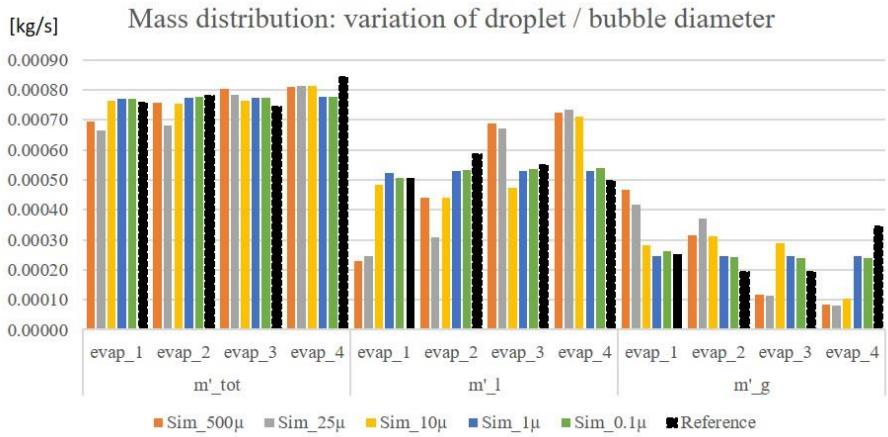

Figure 5: Mass flow distribution (total, liquid and gaseous) due to different droplet / bubble diameters (2)

Basically, in both diagrams the same data values can be seen, but in Figure 4 the differences between each evaporator tube are clearer to understand and in Figure 5 the absolute values are better visible. The results show that no variation of just one droplet / bubble diameter can perfectly reproduce the testbed-data. Small diameters result in a homogenous distribution of the phases and big ones in a non-homogenous distribution. The best representation of the experimental results is given by the smallest droplet diameter of 0.1 µm. In every simulation with larger droplet diameters, the last tube (evap_4) gets the biggest liquid mass fraction, what seems logical because of the rectangular inflow direction to the evaporator tubes and the inertial forces on the droplets. Finally, the inaccuracy of the measurements should also be pointed out here.

4.2 Comparison of different rotations

The testbed is fixed on a frame that can be rotated and because of this setup it is impossible to guarantee a perfect horizontal position for a measurement. In order not to exclude a possible rotation, different small angles of inclination are simulated and compared with the measured, apparently horizontal testbed reference.
The simulated mass distribution on small rotations φ can be seen in Figure 6 and Figure 7 for a total inlet mass flow into the distributor of 11 kg/h with a vapor quality of 0.32. The direction of the rotation is shown in Figure 2.

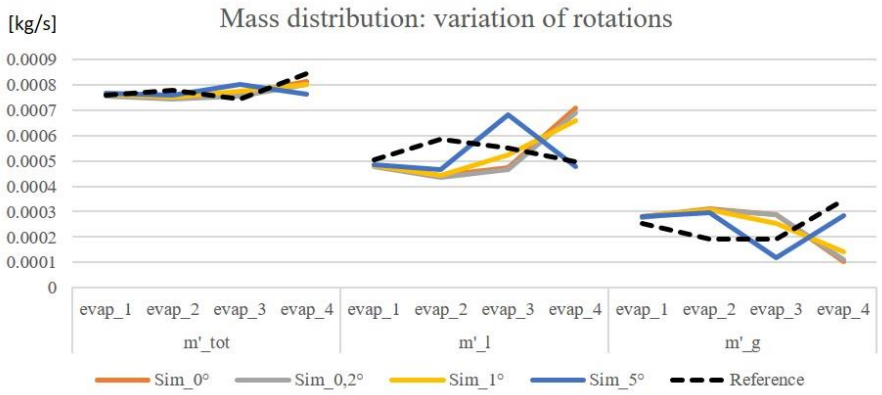

Figure 6: Mass flow distribution (total, liquid and gaseous) due to different angles φ (1)

Small rotations (φ=0.2° and 1°) do not cause a significant trend to fit the measured reference, but with bigger rotations (φ=5°) an improved trend between simulation and measurement can be observed. With the larger rotation, the last evaporator tube (evap_4) does not get the biggest liquid mass fraction anymore. Obviously, the influence of gravity on the liquid mass is already great enough to slow down the droplets and guide them into the middle tubes. It should be noted that a droplet / bubble diameter of 10 µm is applied here. The experiments have been carried out for the horizontal position.

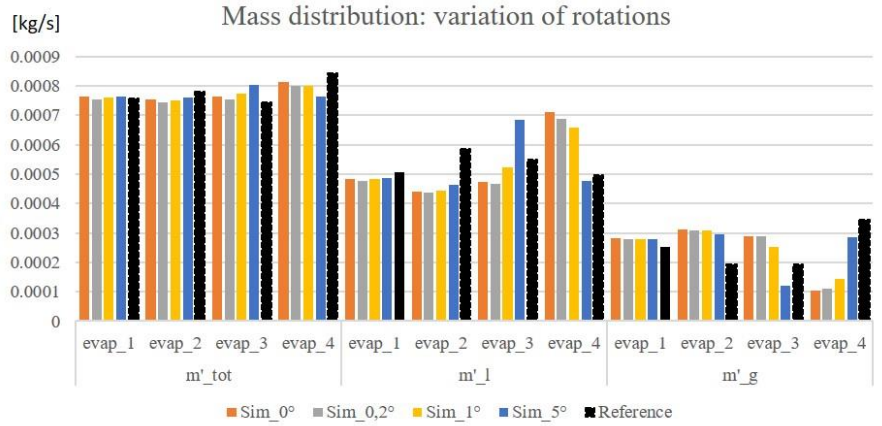

Figure 7: Mass flow distribution (total, liquid and gaseous) due to different angles φ (2)

5 CONCLUSIONS

With the help of the proposed coupling method, it is possible to describe the evaporation process and the corresponding pressure drop and heat transfer of a parallel tube evaporator. The simulations show deviations in the total mass flow distribution in the order of less than 10%. Liquid and vapor mass distribution show larger deviations in the order of 20-50% in different operating conditions. The deviations are related to experimental investigations, which, however, also have only an accuracy of approximately 20%. By describing the evaporation process via the coupling of the 3D and the 1D model, the numerical effort of the simulation is low, which enables an efficient calculation of multi-tube heat exchangers with phase transitions. This method enables an investigation of different operating conditions and geometries on the efficiency of the heat exchanger.
The long-term goal for simulating an evaporator should be a full 3D simulation, but as long as this is not possible due to the computational effort, it makes sense to use a 1D / 3D coupling with a well-estimated error. With this method, important influences on the evaporation process, such as the distribution of the liquid and gaseous mass flows, can be calculated and thus taken into account in the design of the heat exchanger.

NOMENCLATURE

Abbreviations		q	Heat source
1D	One dimensional	$\dot{Q}$	Heat flux
3D	Three dimensional	Re	Reynolds number
AVL	AVL-List GmbH	T	Temperature
C	Programming language	T_e	Excess temperature
CFD	Computational fluid dynamics	v	Velocity
DOE	Design of experiments	x	Quality of specific tube interval
evap_i	Evaporation tube i	**Greek Symbols**	
FIRE	CFD software	α	Heat transfer coefficient
HTC	Heat transfer coefficient	$\nabla\alpha_d$	Difference of volume components
HWT	Hybrid wall treatment	Δ	Delta (Difference)
SWF	Standard wall function	ε	Kinetic dissipation rate
TUG	Graz University of Technology	ρ	Density
VDI	Verein Deutscher Ingenieure e.V.	μ	Viscosity
ViF	Virtual-Vehicle	φ	Angle of inclination
Roman symbols		ϕ	Parameter for pressure loss correlations
A_i	Interfacial area density	**Subscripts**	
Bg	Boiling number	C	Continuous
Bo	Bond number	D	Dispersed
C_D	Drag coefficient	e	Excess
C_{TD}	Constant for dispersion forces	g	Gas
D	Diameter of the tube	go	Gas only
G	Density multiplied by velocity	in	Inlet
G_{MSH}	Parameter for Müller-Steinhagen and Heck correlation	l	Liquid
i	Counting number of tubes	lo	Liquid only
k	Kinetic energy	MSH	Müller-Steinhagen and Heck
k_c	Thermal conductivity of continuous phase	out	Outlet
k_l	Thermal conductivity of liquid	r	Relative
M	Momentum (interfacial exchange)	tot	Total
n	Counting number of discretization elements per tube	tp	Two phase
p	Pressure		

REFERENCES

AVL-List GmbH, 2018. AST-Documentation-FIRE, CFD-Solver. V2018a.release. Graz, Austria.

AVL-List GmbH, 2018. AST-Documentation-FIRE, Eulerian Multiphase. V2018a.release. Graz, Austria.

Bell, C., 2016-2018. fluids: Fluid dynamics component of Chemical Engineering Design Library (ChEDL) https://github.com/CalebBell/fluids.

Bell, C., 2016-2019. ht: Heat transfer component of Chemical Engineering Design Library (ChEDL) https://github.com/CalebBell/ht.

Friedel, L., 1979. Improved Friction Pressure Drop Correlations for Horizontal and Vertical Two-Phase Pipe Flow. in: Proceedings, European Two Phase Flow Group Meeting, Ispra, Italy. 485-481

Kim, S., Mudawar, I., 2012. Universal Approach to Predicting Two-Phase Frictional Pressure Drop for Adiabatic and Condensing Mini/ Micro-Channel Flows. International Journal of Heat and Mass Transfer 55, no. 11-12, 3246-61. doi:10.1016/j.ijheatmasstransfer.2012.02.047.

Kim, S., Mudawar, I., 2014. Review of Databases and Predictive Methods for Pressure Drop in Adiabatic, Condensing and Boiling Mini/Micro-Channel Flows. International Journal of Heat and Mass Transfer 77, 74-97. doi:10.1016/j.ijheatmasstransfer.2014.04.035.

Kollik, C., Ennemoser, A., Lang, M., Almbauer, R., Wimmer, K., Dür, L., Zainer, C., 2021. Experimental Investigation of Liquid and Vapor Mass Flows in a Parallel Tube Evaporator. International Refrigeration and Air Conditioning Conference 18-2623.

Lazarek, G. M., Black, S. H., 1982. Evaporative Heat Transfer, Pressure Drop and Critical Heat Flux in a Small Vertical Tube with R-113. International Journal of Heat and Mass Transfer 25, no. 7, 945-60. doi:10.1016/0017-9310(82)90070-9.

Li, W., Wu, Z., 2010. A General Correlation for Evaporative Heat Transfer in Micro/mini-Channels. International Journal of Heat and Mass Transfer 53, no. 9-10, 1778-87. doi:10.1016/j.ijheatmasstransfer.2010.01.012

Lockhart, R. W., Martinelli, R. C., 1949. Proposed correlation of data for isothermal two-phase, two-component flow in pipes. Chemical Engineering Progress 45 (1), 39-48.

Chisholm, D., 1967. A Theoretical Basis for the Lockhart-Martinelli Correlation for Two-Phase Flow. International Journal of Heat and Mass Transfer 10, no. 12, 1767-78. doi:10.1016/0017-9310(67)90047-6.

Cui, X., Chen, J., 2010. A Re-Examination of the Data of Lockhart-Martinelli. International Journal of Multiphase Flow 36, no. 10, 836-46. doi:10.1016/j.ijmultiphaseflow.2010.06.001.

Müller-Steinhagen, H., Heck, K., 1986. A Simple Friction Pressure Drop Correlation for Two-Phase Flow in Pipes. Chemical Engineering and Processing: Process Intensification 20, no. 6, 297-308. doi:10.1016/0255-2701(86)80008-3.

Stefan, P., Kabelac, S., Kind, M., Mewes, D., Schaber, K., Wetzel, T., 2018. VDI-Wärmeatlas. Springer Vieweg, 12. Edition, Berlin. 978-3-662-52989-8.

Zhang, M., Webb, R. L., 2001. Correlation of Two-Phase Friction for Refrigerants in Small-Diameter Tubes. Experimental Thermal and Fluid Science 25, no. 3-4, 131-39. doi:10.1016/S0894-1777(01)00066-8.

ACKNOWLEDGEMENTS AND FUNDING STATEMENT

This work originated in a project for the development of battery cooling systems in a consortium of the AVL-List GmbH (AVL), Virtual-Vehicle (ViF) and Graz University of Technology (TUG).

The publication was supported by the Virtual Vehicle Research GmbH in Graz, Austria. The authors would like to acknowledge the financial support within the COMET K2 Competence Centers for Excellent Technologies from the Austrian Federal Ministry for Climate Action (BMK), the Austrian Federal Ministry for Digital and Economic Affairs (BMDW), the Province of Styria (Dept. 12) and the Styrian Business Promotion Agency (SFG). The Austrian Research Promotion Agency (FFG) has been authorised for the programme management. They would furthermore like to express their thanks to their supporting industrial and scientific project partners, namely the AVL-List GmbH and to the Graz University of Technology.